LBL--26499

DE90 001420

STOPPING RULES, BAYESIAN RECONSTRUCTIONS AND SIEVES

Jorge Llacer, Eugene Veklerov and Jorge Nunez

Engineering Division, Lawrence Berkeley Lab, Berkeley, CA 94720 U.S.A. (J.L., E.V.) and Department of Physics, University of Barcelona, Barcelona, Spain (J.N.)

INTRODUCTION

During the last two years, our group has been working on the concept of "feasible" images in the context of image reconstruction for emission tomography (ET). The concept has been discussed previously in image processing in astronomy (Skilling and Bryan, 1984; Ables, 1974; Gull and Daniell, 1978; Narayan and Nityananda, 1986) and in information theory (Trussell, 1983; Trussell and Civanlar, 1984; Sezan and Stark, 1982), but had not been applied to tomographic image reconstruction until we related the deterioration of Maximum Likelihood Estimator (MLE) images at large number of iterations to the unfeasibility of the resulting images (Llacer, Veklerov and Hoffman, 1987; Veklerov and Llacer, 1987; Llacer and Veklerov, 1988; Llacer and Veklerov, 1989). We have described a feasible image as an image that, if it were a true radioisotope distribution in a patient, could have generated the measured data by the Poisson process that governs the radioactive decay process. Formal definitions of feasibility, as well as tests that can be applied to computer generated data or to real tomographic data, have been given in the literature cited above.

We consider feasibility necessary but not sufficient for a reconstruction to be acceptable. Indeed, the true radioisotope distribution in a patient is feasible since it did generate the data by a Poisson process. One would then hope that a reconstruction of that distribution is in the same set of feasible images. On the other hand, we have

---

reported feasible images that contain artifacts due to having initiated the iterative process with an inappropriate first guess (Llacer, Veklerov and Nunez, 1989) and we must, therefore, indicate that feasibility is not a sufficient condition for image acceptability.

We have found several ways of obtaining feasible images:

a) by the MLE method stopping the iterations as soon as the images pass our test for feasibility
b) by continuing the iterations past feasibility and returning to it by slight Gaussian filtering
c) by Bayesian methods with entropy prior (Nunez and Llacer, 1989; Nunez and Llacer, 1989a)
d) by the method of sieves (Snyder and Miller, 1985; Snyder et al., 1987)

All the feasible images that we have obtained are different from each other in some subtle ways. For the case of MLE reconstructions, H. Barrett (private communication), suggested that cutting the MLE iterative process short of maximizing the likelihood function may result in the loss of image eigenvectors corresponding to small eigenvalues. We have examined methods of characterizing the differences among the different feasible images and it will be the objective of this paper to discuss the preliminary results of our efforts in that direction.

RECONSTRUCTION METHODS

We will discuss results from the four different methods of obtaining feasible images listed above, starting in all cases from one single set of projection data from the ECAT-III tomograph of UCLA (Hoffman et al., 1983) in a measurement of the Hoffman brain phantom. Most of the reconstructions have been carried out with transition matrices calculated by the simple Shepp-Vardi prescription of 1982 and also with Monte Carlo generated matrices that take into consideration detector geometry, detector material properties, positron range and cross-talk (Veklerov, Llacer and Hoffman, 1988). Random coincidences and background have been subtracted previous to the reconstruction and corrections due to absorption and detector gain have been made to the data for the MLE case and to the matrix for the Bayesian and sieve methods.

The number of variations that can be expected from all the possible combinations of processing steps is excessive for a reasonable presentation. A careful examination of the results allows, however, to draw some preliminary conclusions about the major observed differences in the results. They are preliminary in the sense that they are based on only one instance of the projection data and need, therefore, to be repeated adequately for verification.

The FMAPE Method

Of the reconstruction methods indicated above, the one that is least known is the FMAPE, for Fast Maximum a Posteriori with Entropy (Nunez and Llacer, 1989a). It will be described here briefly.

The notation that we are using is the following:

p_j $j = 1,\ldots,D$ - the projection data or the number of counts

a_i $i = 1,\ldots,B$ - the radioisotope activity or emission density

f_{ji} - transition matrix elements, or probability that a disintegration in box i will be detected in tube j.

$h_j = \sum_{i=1}^{B} f_{ji}\, a_i$ - the forward projection

The FMAPE is a Bayesian method based on maximizing the target function

$$BY = -\sum_{i=1}^{B} (a_i/\Delta a)\, \log(a_i/\Delta a) + \sum_{j=1}^{D} [-h'_j + (p^*_j/\Delta p_j)\, \log(h'_j)] - \mu \left(\sum_{i=1}^{B} a_i - N \right) \qquad (1)$$

where

$$h'_j = \left(\sum_{i=1}^{B} f_{ji} \; a_i \right) / \Delta p_j \, , \qquad j = 1,\ldots,D \qquad (2)$$

The first term is the Shannon entropy with one adjustable parameter, Δa, which controls the relative weight of the entropy vs. likelihood. It can be adjusted to yield reconstructions that converge to feasible images. The second term is the likelihood which contains a vector of projection data p^*_j incorporating absorption and detector gain corrections and a vector of those corrections Δp^*_j. The third term insures the conservation of counts and contains one Lagrange multiplier μ. The vector of elements h'_j corresponds to a modified projection of the current image a_i and, in fact, prescribes that the corrections be applied to the matrix elements f_{ji}. The iterative algorithm we have devised for the maximization is based on the "successive substitutions" method (Hildebrand, 1974) and is given by

$$a_i^{k+1} = K \, a_i^k \cdot$$

$$\left\{ \Delta a \sum_{j=1}^{D} \left(f_{ji} (1/\Delta p_j) \left[(p^*_j / \sum_{i=1}^{B} f_{ji} a_i^k) - 1 \right] \right) - \log(a_i^k) + C \right\}^n$$

$$i = 1,\ldots,B \qquad (3)$$

There are two constants in Eq. 3 whose values are arbitrary. Within the range of values for which the iterative process converges, the convergence point is independent of their value. The first constant is the exponent n which controls the speed of convergence. We have found that for values $1 \leq n \leq 3$, the rate of convergence is roughly proportional to n. The second is the constant C, which insures that no negative values will occur during the iterative process. We use routinely $C = \Delta a$ with no problems. Finally, K is computed at the end of each iteration to conserve the number of counts and it is equivalent to calculating the Lagrange multiplier μ by

$$K = 1 \; / \; \{ \; 1 + \Delta a \; \mu - \log(\Delta a) + C \}^n \qquad (4)$$

The Method of Sieves

We have studied the method of sieves proposed by Snyder and Miller for the regularization of MLE reconstructions (Veklerov and Llacer, 1989) for the purpose of finding whether a proper selection of the value for the sieve kernel width would result in feasible reconstructions. The results have been positive and the initial arbitrariness in the choice of that parameter can now be removed by the feasibility requirement. From the computational point of view, the method of sieves consists in an MLE iterative procedure like that of Shepp and Vardi, with the difference that the transition matrix f_{ji} is pre-convolved with a Gaussian kernel with parameter ß, controlling the smoothness of the final result. In the notation of the present paper, the recursive formula is

$$a_i^{(k+1)} = a_i^{(k+1)} \sum_{j=1}^{D} \left[g_{ji}\, p_j \Big/ \sum_{i=1}^{B} g_{ji}\, a_i^{(k)} \right] \qquad i = 1,\ldots,B. \tag{5}$$

where

$$g_{ji} = \sum_{m=1}^{B} f_{jm}\, K_{mi}$$

is the convolution with a Gaussian kernel K. After the iterative procedure has converged, the final image is obtained from

$$a_i = \sum_{m=1}^{B} a_i^{(k)}\, K_{mi}. \tag{6}$$

A small amount of experimentation with the parameter ß of kernel K yielded feasible images for both computer generated and real data.

IMAGE EVALUATION PROCESS

A basis for comparison of different reconstruction results of phantom images should be the phantom itself. With data from a real tomograph, however, the finite size of the detector elements will invariably result in projection data in which the frequency response of the instrument will limit the fidelity with which the phantom can be reproduced. It appears, then, that the comparison of reconstruction results should be made with the "best" image that the tomograph can generate under ideal circumstances. For that purpose, we have used a data set with 55 million counts (55M) and used a filtered backprojection algorithm with the Shepp-Logan filter (FBP), providing very sharp results and acceptably low noise. Because of the linearity of the FBP method, we expect the activity values obtained in the two regions-of-interest (ROIs) that have been chosen for bias comparisons (shown in Fig. 1a) to be a good representation of the ratio of hot vs. cold activity levels in the phantom. The size of the ROIs is large enough to include many pixels, located within image features much larger than the point response of the instrument.

The FBP method assumes that the tomograph point response function is space invariant. All the methods we have used to obtain our feasible reconstructions are based on transition matrices corresponding to non-space invariant response functions. A pixel-by-pixel comparison between the FBP results and those of the tested methods, in configuration space as well as in frequency or Hilbert space, results in failure by misregistration. Even comparisons between results of the Shepp-Vardi and the Monte-Carlo matrices suffer from that effect, by as much as one pixel at the phantom edges. For that reason, we have limited our pixel-by-pixel comparisons to within the groups of reconstructions using the same transition matrices. Inter-group comparisons, or comparisons with the FBP results, have been carried out only for major features in the phantom.

The question of whether it would be of advantage to carry out comparisons through Fourier transforms, eigenimages or eigenanalysis based on the eigenvectors of the transition matrices has been studied. The difficulty encountered by not being able to identify differences in the "frequency" domain as being differences in noise or in high frequency image features appears to render transform methods less useful, at this time, than work done in configuration space, which is what we have done.

PRELIMINARY RESULTS AND DISCUSSION

We present here our preliminary observations, based on one single data set of 1 million (1M) counts. All the reconstructions have been normalized to 80% activity corresponding to the average of the high activity ROI shown in Fig. 1. Subtractions on a pixel-by-pixel basis have been carried out bi-directionally, with negative values suppressed. The difference images have been displayed in a color scale 10 times (X 10) more sensitive than the scale used to display the normal reconstructions. The abbreviations used to denominate the different reconstruction methods are the following:

MLE.SR: Maximum Likelihood Estimator, stopped according to our Stopping Rule at the onset of feasibility

MLE.PF: MLE, stopped at a point with 60% more iterations than MLE.SR, and Post-Filtered with a Gaussian kernel of σ = 0.7 to 0.8 pixels

FMAPE.PF: FMAPE reconstruction, with Δa chosen for convergence past feasibility, with Post-Filtering as above

SIEVE: Reconstruction by the method of sieves, with parameter β chosen so that process converges to a feasible image

The results that will be discussed here are for reconstructions with the Shepp-Vardi (SV) matrix. In general, the reconstructions obtained with the Monte Carlo matrices do not show any visible differences from the SV results, although profiles taken through the MC images indicate sharper results.

Effect of Iterating Past Feasibility and Post-Filtering

Figures 1a), b), c) and d) show, respectively, the MLE.SR and MLE.PF results and the X 10 differences between the two images. The differences between 1a) and 1b) are too small to be noticeable in the printed image. This is a characteristic of all our results and, for that reason, the reconstruction results will not generally be shown.

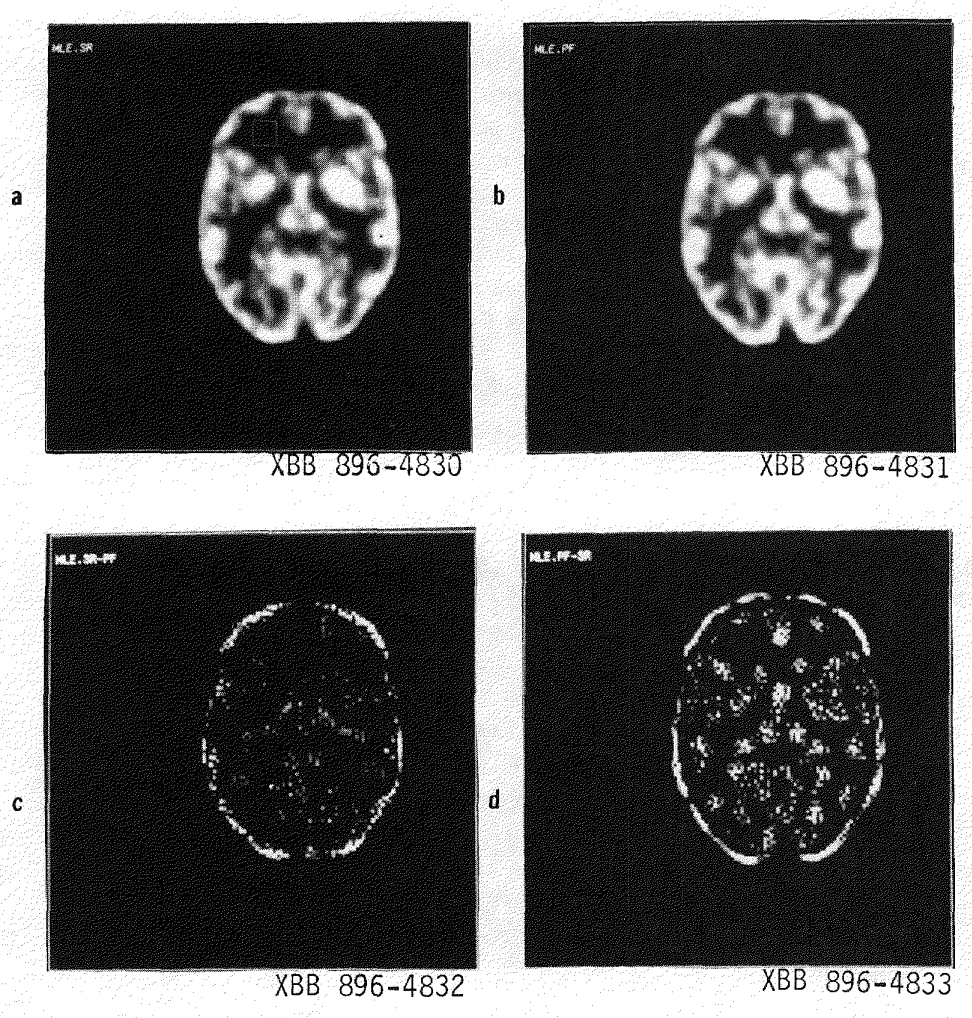

Fig. 1 - Reconstructions of a data set with 1 million counts by the MLE method. a) Stopping at the onset of feasibility, at iteration 30 (SR), b) Continuing to iteration 50 and post-filtering with a Gaussian kernel of $\sigma = 0.8$ pixels (PF), c) Difference (SR-PF), magnified X 10, negative values set to zero, d) Difference (PF-SR), same conditions as c).

The difference image SR-PF shows pixel values in which the SR image has higher values than those of the PF image and vice-versa for the PF-SR image. The phantom periphery is clearly visible in both cases and it is due principally to the broadening and flattening effect of the Gaussian post-filtering in the PF image. In SR-PF of Fig.

1c), the most significant visible features are faintly visible narrow valleys and in PF-SR of Fig. 1d), the most prominent features are the smaller hot regions of the phantom.

The interpretation of the difference images is that iterating past the onset of feasibility results in the narrow valleys of the phantom becoming deeper and the smaller hot regions becoming higher, i.e., increasing the contrast for small features. The ratio of hot to cold ROIs of Fig. 1a) is 4.32 for the 55M FBP results, 4.50 for the SR and 4.74 for the PF results. This number fluctuates in all the reconstructions with 1M counts between a low of 4.0 for the FMAPE reconstructions and a high of 5.17 for the sieve results. Similar effects are obtained by comparisons within the set of MLE results obtained with the MC matrix or with the FMAPE results converging to just feasibility or past feasibility and post-filtering.

Comparison Between MLE.PF and Bayesian FMAPE Results

Figure 2a) shows the difference between MLE and FMAPE results, both with post-filtering, and the Shepp-Vardi matrix. Only a few hot spots appear, indicating that the FMAPE has reduced the size of some of the "unstable" points of the MLE reconstruction. Figure 2b) shows the FMAPE - MLE difference which shows a bias in the complete low activity part of the phantom, with the FMAPE yielding an estimate which is higher than the MLE by approximately 3% of the maximum activity. In spite of misregistration problems, it is possible to compare the FMAPE and MLE results with the FBP reference. The suspected bias of the FMAPE is confirmed by that comparison. However, comparing MLE.PF results with FMAPE with the parameter Δa chosen so that the method converges substantially past feasibility (Δa =800, instead of 400) and postfiltering yields an almost complete correction of the observed bias.

Comparison Between MLE and SIEVE Results

A comparison between MLE.SR or MLE.PF and sieve results indicates that the sieve results are too low in the regions of low activity by approximately 2% with respect to the MLE, making the ratio of high to low activity ROIs of Fig. 1a) the highest measured in the present experiments. In addition, it appears that the sieve results are too high

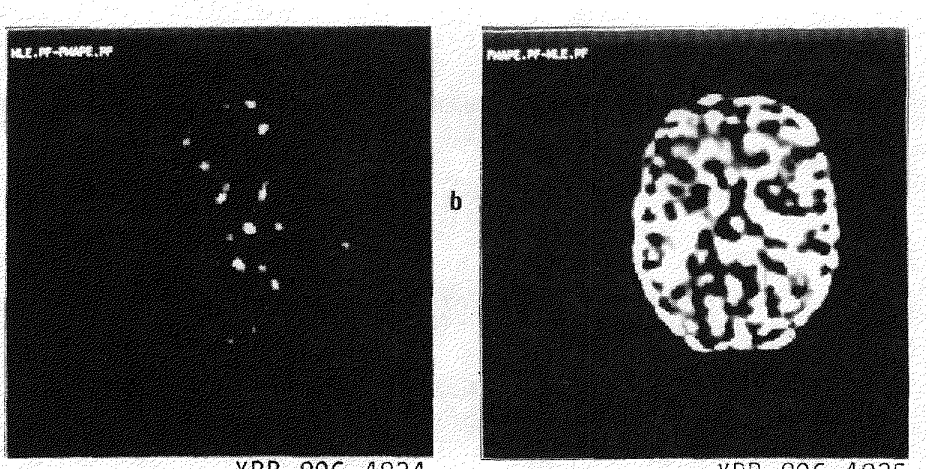

Fig. 2 - Differences magnified X 10, between MLE with post filtering (MLE.PF) and Bayesian reconstruction with the FMAPE algorithm (FMAPE.PF). a) MLE-FMAPE and b) FMAPE-MLE. In both cases negative values have been set to zero.

in regions of small hot features, or at edges, and too low in narrow valleys, i.e., it appears to suffer from ringing. This effects are seen in the X 10 difference images of Figs. 3a) and b). The ringing effect has already been observed by Snyder et al. and they have proposed the use of a "resolution kernel" in the reconstruction. We have implemented it approximately by a Gaussian post-filtering operation with the same kernel that we have used for the MLE results (σ = 0.8 pixels). The differences between post-filtered images are almost featureless and we conclude that the two images are essentially equivalent, although the ratio of ROIs for the sieve image is still too high.

We have also measured the ratio of ROIs in the FBP.SL reconstruction for the 1M count data set used in the above reconstructions and we have found it to be 4.31, essentially the same as with 55M counts.

CONCLUSIONS

The work described above confirms our early visual observation that not all feasible images are equivalent in terms of their possible medical content. We could rank the three main methods of reconstruction investigated in order of the range of values that they exhibit:

1) FMAPE reconstructions, with average values in large ROIs that are too compressed, by ~ 3% of the maximum, except when parameter Δa is chosen for convergence substantially past feasibility

2) MLE reconstructions, that have ROI values that are somewhat expanded, within 1 - 2% of the correct range

3) Sieve methods that show a range of ROI values that is expanded by approximately 3%, although this effect has to be checked after incorporating the resolution kernel into the algorithm

We realize that these conclusions are based on an analysis of reconstructions from only one set of data and that it is necessary to verify them by reconstructing more sets of data. We have just initiated that process.

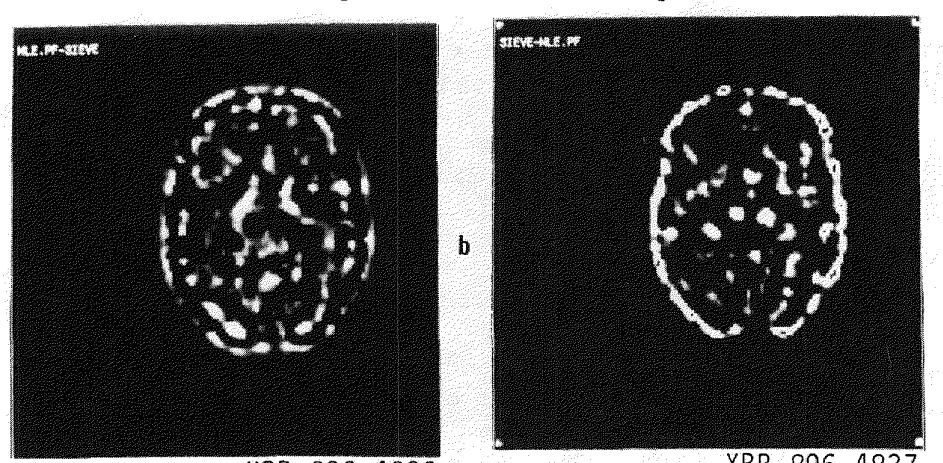

Fig. 3 - Differences magnified X 10 between MLE reconstructions with post-filtering (MLE.PF) and sieve results, unfiltered.

All the feasible images that we have obtained are visually good, with the sieve images (without post-filtering) being the most pleasing ones (smoother, higher contrast).

The work that we have reported is preliminary to the selection of one or two main reconstruction methods for an extensive ROC analysis of the possible benefits of statistically based algorithms in PET in collaboration with the Nuclear Medicine Group at UCLA.

ACKNOWLEDGMENTS

This work has been supported, in part, by a grant from the National Institutes of Health, CA-39501 and by the U.S. Department of Energy under Contract No. DE-AC03-76SF00098. Dr. Nunez' work was supported, in part, by the Center of Catalan Studies, Generalitat de Catalunya, Spain and University of California, Berkeley.

REFERENCES

Ables JG (1974). Maximum entropy spectral analysis. Astron. Astrophys. Suppl. 15:383-393.

Gull SF, Daniell GJ (1978). Image reconstruction from incomplete and noisy data. Nature 272:686-690.

Hoffman EJ, Ricci AR, van der Stee LMAM, Phelps ME (1983). ECAT-III - basic design considerations. IEEE Trans. Nucl. Sci. NS-30:729-733.

Llacer J, Veklerov E, Hoffman EJ (1987). Convergence of the maximum likelihood estimator method of tomographic image reconstruction. Proc. SPIE, Medical Imaging 767:70-76.

Llacer J, Veklerov E (1988). The maximum likelihood estimator method of image reconstruction: its fundamental characteristics and their origin. Information Processing in Medical Imaging, de Graaf and Viergever, eds., Plenum:201-217.

Llacer J, Veklerov E (1989). Feasible images and practical stopping rules for iterative algorithms in emission tomography. IEEE Trans. Med. Imaging MI-8:186-193.

Llacer J, Veklerov E, Nunez J (1989). The concept of causality (feasibility) in image reconstruction. NATO Advanced Study Institute, Povoa, Portugal, Sept. 1988. Proc. to be publ.

Narayan R, Nityananda R (1986). Maximum entropy image restoration in astronomy. Ann. Rev. Astron. Astrophys. 24:127-170.

Nunez J, Llacer J (1989). Maximum entropy and the concept of feasibility in tomographic image reconstruction. SPIE Medical Imaging III: Image Formation 1090:359-372.

Nunez J, Llacer J (1989a). A fast Bayesian reconstruction algorithm for emission tomography with entropy prior converging to feasible images. LBL-27074. To be publ.

Sezan MI, Stark H (1982). Image restoration by the method of convex projections: Part 2 - Applications and numerical results. IEEE Trans. Med. Imaging, MI-1.

Skilling J, Bryan RK (1984). Maximum entropy reconstruction: general algorithm. Monthly Notices of the Royal Astronomical Soc. 211:111-124.

Snyder DL, Miller MI (1985). The use of sieves to stabilize images produced with the EM algorithm for emission tomography. IEEE Trans. Nucl. Sci.,NS-32:3864-3872.

Snyder DL, Miller MI, Thomas LJ, Politte DA (1987). Noise and edge artifacts in maximum-likelihood reconstructions for emission tomography. IEEE Trans. Med. Imaging MI-6.

Trussell HJ (1983). Convergence criteria for iterative restoration methods. IEEE Trans. Acoust., Speech, Signal Processing ASSP-31.

Trussell HJ, Civanlar MR (1984). The feasible solution in signal restoration. IEEE Trans. Acout., Speech, Signal Processing ASSP-32.

Veklerov E, Llacer J (1987). Stopping rule for the MLE algorithm based on statistical hypothesis testing. IEEE Trans. Med. Imaging MI-6:313-319.

Veklerov E, Llacer J, Hoffman EJ (1988). MLE reconstruction of a brain phantom using a Monte Carlo transition matrix and a statistical stopping rule. IEEE Trans. Nucl. Sci. NS-35.